

Measurement of Neutral- and Charged-Pion Form-Factor Slopes*

S. DEVONS, P. NÉMETHY,† AND C. NISSIM-SABAT‡
Columbia University, New York, New York

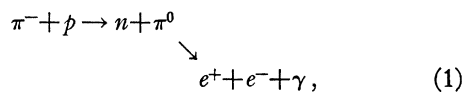
AND

E. DI CAPUA AND A. LANZARA
Istituto di Fisica dell'Università, Rome and Istituto Nazionale di Fisica Nucleare, Sezione di Roma, Italy
(Received 14 January 1969)

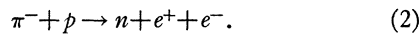
In an experiment performed at Columbia University's Nevis cyclotron, we studied the reactions (1) $\pi^0 \rightarrow \gamma + e^+ + e^-$ and (2) $\pi^- + p \rightarrow n + e^+ + e^-$ for π^- at rest. Using a system of counters and spark chambers, we selected pairs with an opening angle near 120° . We analyzed the invariant-mass spectrum of the pairs (1) in 2200 π^0 decays and (2) in 400 radiative captures. For the π^0 form-factor slope, we find $a = (+0.01 \pm 0.11)/m_\pi^2$. We obtain the charged-pion form-factor slope for time like momentum transfers of the order of m_π . Our result for the pion charge radius is $r_\pi < 1.9$ F with a 90% confidence level.

1. INTRODUCTION

FROM the capture of π^- mesons at rest in liquid hydrogen, we observed two processes: the production of a Dalitz pair in π^0 decay,



and the internal conversion of the γ ray in radiative capture,



Process (1) can be described by the Feynman graph of Fig. 1. The form factor for the vertex $\pi^0\gamma\gamma$, called the electromagnetic form factor of the π^0 , is a function $\Gamma(x)$ of the virtual photon mass squared, that is of the invariant mass squared x of the electron-positron pair. $\Gamma(x)$ appears as a factor in the amplitude of the Dalitz decay (1); $[\Gamma(x)]^2$ is the factor in the x distribution of the pairs. It has been pointed out¹ that, for values of x of the order of m_π^2 , the form factor could produce observable deviations of the x spectrum from the distribution predicted on a purely electrodynamic basis.^{2,3} We use the normalization $\Gamma(0) = 1$. The nearest singularities in the form factor $\Gamma(x)$ are associated with multipion intermediate states. Because we are well below the threshold for these, a first-order approximation,

$$\Gamma(x) = 1 + ax,$$

is sufficient,¹ and the form-factor slope a is the parameter to be measured.

Several theoretical estimates of a , based on dispersion relations⁴⁻⁶ or on the vector-dominance model,⁷

* This work was supported in part by the Office of Naval Research.

† Now at Saclay Laboratory, Gif-sur-Yvette, France.

‡ Northeastern Illinois State College, Chicago, and E. Fermi Institute, University of Chicago.

¹ S. M. Berman and G. A. Geffen, *Nuovo Cimento* **18**, 1192 (1960).

² N. M. Kroll and W. Wada, *Phys. Rev.* **98**, 1355 (1955).

³ D. Joseph, *Nuovo Cimento* **16**, 997 (1960).

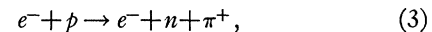
⁴ H. S. Wong, *Phys. Rev.* **121**, 289 (1961).

have been published. All the predictions agree on a small positive value of a in the range of 0.02 to 0.05 m_π^{-2} . In particular, the assumption of ρ dominance gives as a form factor $\Gamma(x)$ the ρ propagator

$$\frac{1}{1 - x/m_\rho^2}$$

corresponding to a slope $a = 0.03 m_\pi^{-2}$. Samios⁸ and Kobrak⁹ measured a in two independent experiments with hydrogen bubble chambers. Both experiments gave large negative values of a . Even though the experimental errors were large, the results were in substantial disagreement with the theory. This situation was the main reason for doing the present experiment, which employs a different technique.

The radiative-capture process (2) can be described by the graph of Fig. 2 with a virtual photon of time-like four-momentum, corresponding to a positive invariant mass x for the pair. The same graph describes the related process



which can be considered as the photoproduction of a π^+ by a spacelike virtual photon. Therefore, processes (2) and (3) are complementary in the sense that both yield information on the same form factors but in opposite ranges of x . While the resonance $N_{3/2}^*$ gives a dominant contribution to the electroproduction process (3), it does not contribute at all to our radiative capture process, because the π^- is captured in $> 99\%$ of the cases in the S wave.¹⁰ The relevant form factor here is, besides the rather well-known nucleon form factors, the electromagnetic form factor $F_\pi(x)$ of the charged pion,^{11,12} which describes a $\pi\pi\gamma$ vertex. Again

⁵ D. A. Geffen, *Phys. Rev.* **128**, 374 (1962).

⁶ G. Barton and B. G. Smith, *Nuovo Cimento* **36**, 436 (1965).

⁷ M. Gell-Mann and F. Zachariasen, *Phys. Rev.* **124**, 953 (1961).

⁸ N. P. Samios, *Phys. Rev.* **121**, 275 (1961).

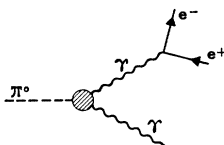
⁹ H. Kobrak, *Nuovo Cimento* **20**, 115 (1961).

¹⁰ M. Leon and H. A. Bethe, *Phys. Rev.* **127**, 636 (1962).

¹¹ A. Lanzara, thesis, University of Rome, 1966 (unpublished).

¹² B. De Tollis and F. Nicolo, *Nuovo Cimento* **48A**, 281 (1967).

FIG. 1. Diagram for the decay $\pi^0 \rightarrow e^+ + e^- + \gamma$.



its effects appear in the x spectrum of the pair in radiative capture (2), but in a more intricate way than $\Gamma(x)$ in Dalitz decay (1). In the range of $x \leq m_\pi^2$ we can again use a one-parameter description of the form factor,

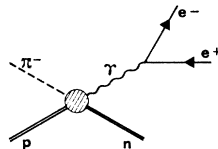
$$F_\pi(x) = 1 + bx.$$

As for the π^0 , the ρ -dominance model predicts for the form-factor slope the value $b = 0.03 m_\pi^{-2}$ associated with the ρ propagator.

Measurements of F_π exist for the region of spacelike momentum transfers, by π^+ electroproduction^{13,14} and by π -He scattering.^{15,16} However, there were no previous results for timelike momentum transfers until the recent experiments produced $\pi^+\pi^-$ pairs with e^+e^- colliding beams.^{17,18} These experiments scanned the region of the ρ resonance, while our radiative capture process explores the region $x \leq m_\pi^2$. The two bubble-chamber experiments quoted above^{8,9} could not give information on F_π , because they were not sensitive enough to the contribution of longitudinally polarized photons to the graph of Fig. 2. It has been shown¹¹ that the pion form factor does not affect the dominant transverse photon contribution.

The present experiment, with the number of events substantially smaller than the aggregate of the bubble-chamber experiments, is nevertheless more sensitive to form-factor effects, both in channel one and in channel two. This has been accomplished essentially by the

FIG. 2. Diagram for the radiative capture $\pi^- + p \rightarrow n + e^+ + e^-$.



¹³ C. W. Akerlof, W. W. Ash, K. Berkelman, A. C. Liechtenstein, A. Romanianskas, and R. H. Siemon, *Phys. Rev.* **163**, 1482 (1967).

¹⁴ C. Mistretta, D. Imrie, J. A. Appel, R. J. Budnitz, L. Carroll, M. Goitein, H. Kanson, and R. Wilson, *Phys. Rev. Letters* **20**, 1523 (1968).

¹⁵ M. E. Nordberg, Jr., and K. F. Kinsey, *Phys. Letters* **20**, 692 (1966); M. M. Block, I. Kenyon, J. Keren, D. Koethke, P. Malhotra, R. Walker, and H. Wenzeler, *Phys. Rev.* **169**, 1074 (1968).

¹⁶ K. M. Crowe, A. Fainberg, J. Miller, and A. S. L. Parsons, *Phys. Rev.* (unpublished).

¹⁷ V. L. Auslander, G. I. Budker, Ju. N. Pestov, V. A. Sidorov, A. N. Skrinsky, and A. G. Khabakhpashev, *Phys. Letters* **25B**, 433 (1967); see also S. C. C. Ting, in *Proceedings of the Fourteenth International Conference on High-Energy Physics, Vienna, 1968* (CERN, Geneva, 1968), p. 43.

¹⁸ J. E. Augustin, J. C. Bizot, J. Buon, J. Haissinsky, D. Lalanne, P. S. Marin, H. Nguyen Ngoc, J. Perez-y-Jorba, F. Rumpf, E. Silva, and S. Tavernier, in *Proceedings of the Fourteenth International Conference on High-Energy Physics, Vienna, 1968* (CERN, Geneva, 1968); see S. C. C. Ting (Ref. 17).

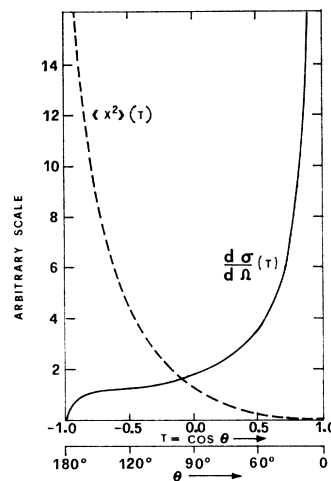


FIG. 3. Angular distribution of Dalitz pairs in π^0 decay (solid line), and of the mean value of x^2 .

selection of electron-positron pairs with an opening angle near 120° , by means of a counter and spark-chamber system. In fact, in both channels the large values of x , for which the form factor can deviate appreciably from unity, are possible only with large-angle pairs. In particular, for the Dalitz decay of the $\pi^0(1)$ the total x distribution on the pairs is sharply peaked for x near zero. By our selection of events with large opening angle we change the shape of the observed x spectrum. Whatever the shape of this spectrum, the minimum statistical error in an estimate of a is given by $\sigma \simeq (N \langle x^2 \rangle_{av})^{-1/2}$ for a sample of N events. Figure 3 shows the dependence of $\langle x^2 \rangle_{av}$ on the selected opening angle θ , together with the angular distribution. With increasing opening angle there is a significant rise of $\langle x^2 \rangle_{av}$ and a steady drop in rate. In order to maximize the statistical accuracy we would like the biggest

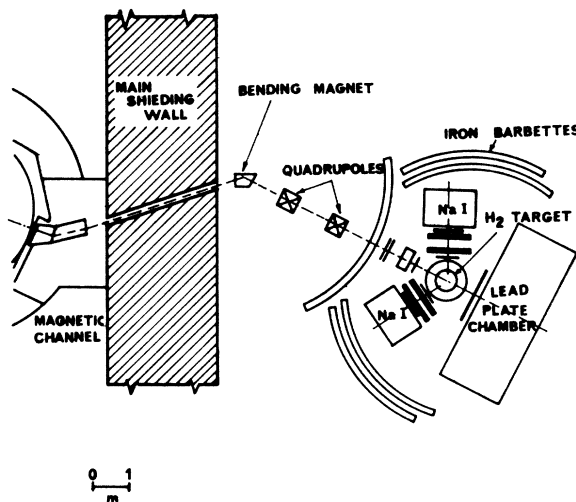


FIG. 4. Layout of the experiment on the cyclotron floor.

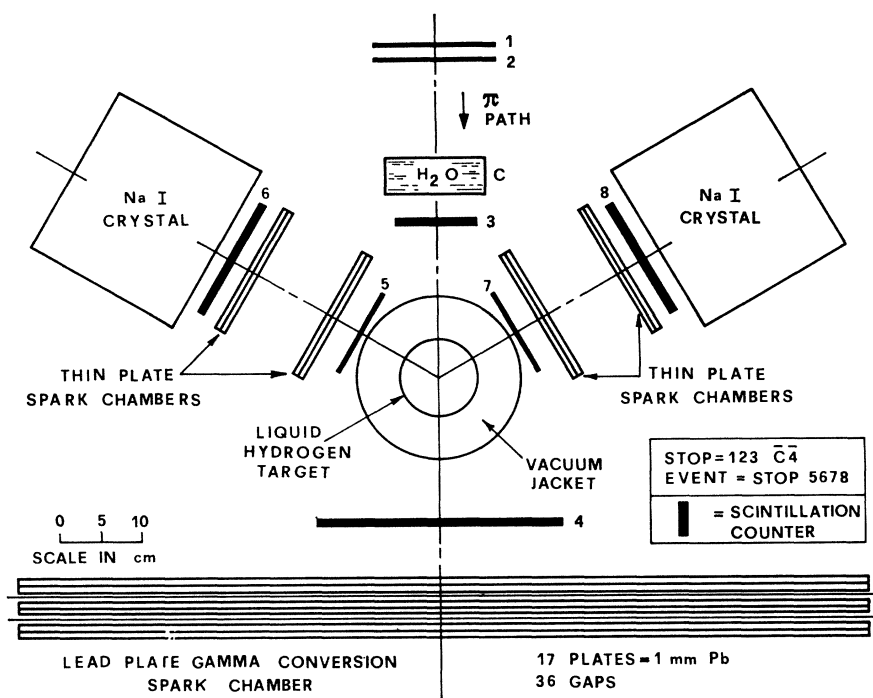


FIG. 5. Schematic diagram of target and detectors.

possible opening angle. Because of the experimental requirements of defining the vertex and of observing the γ ray, we choose an angle of 120° .

Similarly, for the radiative capture reaction (2) the ratio of longitudinal to transverse contribution is enhanced by a factor of 8 for our selected pair opening angle. At the same time our choice of large x increases the sensitivity to any deviation of form factor F_π from 1 and therefore our sensitivity to its slope b .

2. EXPERIMENTAL DETAILS

The layout of the experiment and the arrangement of the target and detectors are shown in Figs. 4 and 5. A 150-MeV/ c beam, produced at Columbia University's Nevis Cyclotron, is defined by a beam telescope, moderated in an absorber, and stopped in a liquid-hydrogen target. Part of the moderator is a 5-cm-thick water Čerenkov counter which rejects electrons with 92% efficiency. Figure 6 shows the target, a thin-walled Mylar cylinder, 10 cm in diameter. Viewing the target are two scintillation-counter telescopes whose axes define an angle of 120° . The aperture of each electron telescope is 1.5% of the sphere. An event trigger is defined as a π^- stop in coincidence with a charged particle in each electron telescope.

The trigger fires thin-plate spark chambers which record electron trajectories. Behind each telescope is a large sodium iodide crystal scintillator, 22 cm in diameter and 22 cm long. These total absorption spectrometers measure the electron and positron energy; their pulse heights are digitized by two 400-channel R. I. D. L. analyzers gated by the event trigger. The

resolution curve of the spectrometers is plotted in Fig. 7. Opposite the electron telescopes is a large lead-plate spark chamber that converts a fraction of the γ 's from π^0 decay (1). The size of the plates is $60 \times 90 \times 0.1$ cm; the total depth of the chamber is 3.5 radiation lengths.

The entire information on each event is photographed on 35-mm film. The total number of pions stopped in the target is 1.3×10^{10} . With a stop rate of 10^4 /sec we have an event trigger about once per minute. Of our 22 000 photographs about one-third are associated with real events (1) or (2).

In between events both analyzers store γ -energy spectra from the dominant reactions $\pi^0 \rightarrow \gamma + \gamma$ and $\pi^- + p \rightarrow n + \gamma$. To get a trigger associated with these γ 's we convert them in thin lead sheets mounted in front of counters 6 and 8 (Fig. 5). Spark-chamber, counter, and coincidence-circuit efficiencies are measured periodically, and the gain of the phototubes is adjusted once a day.

We spent a total of 12 weeks on the cyclotron floor. Of this time slightly less than half was used to produce events.

3. ANALYSIS

The kinematical variables describing the final state in reaction (1) or (2) are the invariant mass squared of the electron-positron pair x and the energy partition $y = (E_+ - E_-) / |\mathbf{p}_+ - \mathbf{p}_-|$ in the c.m. system. For the Dalitz decay (1) all information on the form factor is contained in the spectrum of x alone, since $[\Gamma(x)]^2$ appears simply as a factor in the pair distribution. For the radiative capture (2) this is not true. However, for

Fig. 6. Construction of the hydrogen target.

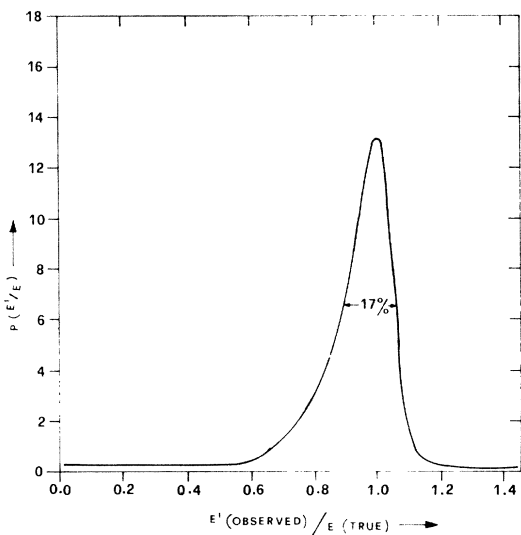
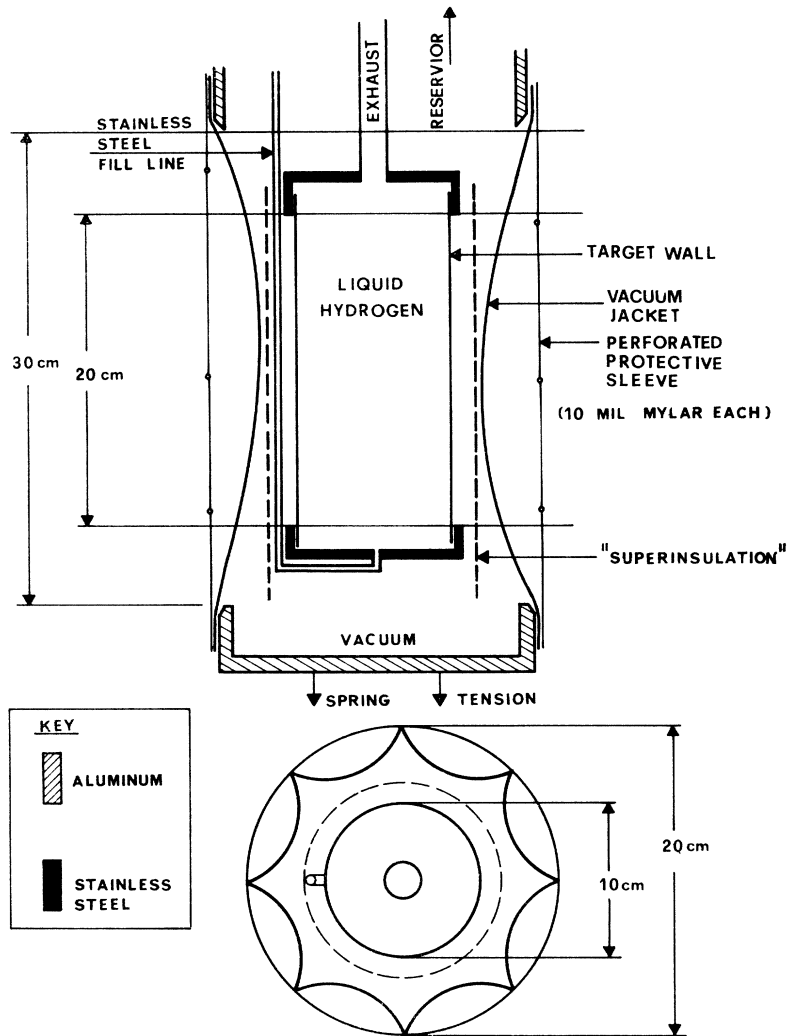


Fig. 7. Resolution function of the sodium iodide crystal spectrometer obtained experimentally.

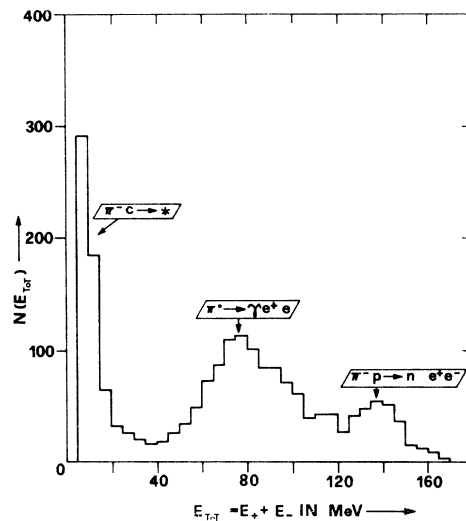


Fig. 8. Histogram of the total energy of the charged pair for a sample of pictures, with no cuts.

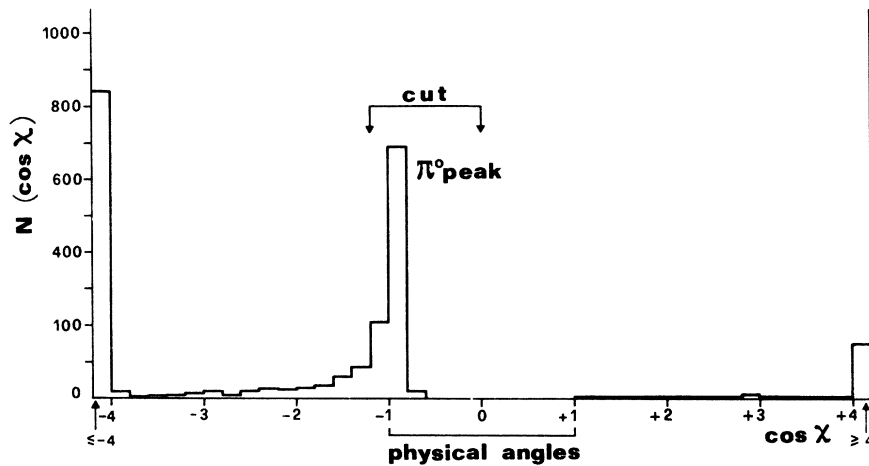


FIG. 9. Histogram of $\cos\chi$ predicted for a sample of pictures, with no cuts.

our experimental events, selected in a small range, of pair opening angles, the two variables x and y are strongly correlated. Thus, we may again obtain all the information we are interested in from the one-dimensional spectrum of x .

The first step of the analysis is the geometric reconstruction, with a rejection of all events with the vertex of the pair outside of a fiducial region in the target or with a poor vertex definition.

Kinematical reconstruction follows. As we already pointed out, the spectrometer gain (channels/MeV) is calibrated from the γ spectra stored in each analyzer. Energies of the electrons are reconstructed taking into account the energy losses.

The third step is the separation of π^0 decays from the radiative-capture events and of both from any kind of background. This is accomplished by taking appropriate cuts in the $E_{\text{tot}} = E_+ + E_-$ spectrum and in the distribution of the predicted cosine of the angle χ between the total momentum of the pair and the γ ray from $\pi^0 \rightarrow e^-e^+\gamma$, as calculated from the measured electron variables E_+ , E_- , and θ . In the E_{tot} spectrum the processes (1) and (2) produce two distinct peaks (Fig. 8), while the main contamination, stars from capture in carbon, is limited to the very low total energy region. The distribution of the calculated $\cos\chi$ has a peak near the value -1 for genuine π^0 decays, while it is essentially flat between plus and minus infinity both for carbon-associated stars and for radiative-capture events (Fig. 9). After our cuts there remains in our sample of π^0 decays a contamination of $(1.9 \pm 0.3)\%$ from radiative capture and $(9.1 \pm 1.2)\%$ from carbon stars. This background can be completely suppressed if we require the observation of the real γ ray in the γ -conversion spark chamber. The residual contamination of π^0 decay events in our sample of radiative captures is $(11.2 \pm 0.2)\%$. Other contamination sources were carefully considered and were found to be negligible. Out of 10 000 events that passed the geometric reconstruction we get 2200 π^0 decays (of which 997

have a converted γ) and 800 radiative-capture events. The sample of the latter is further reduced by a cut on the individual energies measured. This cut is necessary because of uncertainties in a saturation effect of the phototubes looking at the NaI crystal; the saturation gives a nonlinear response in the region of very high energies. After this cut we remain with 400 pairs from the radiative-capture reaction.

At this point we construct an experimental x spectrum for both channels (1) and (2). As a function of the measured variables, x is given by $x \approx 2E_+E_-(1 - \cos\theta)$. Then we confront the experimental spectrum with the theoretical one. The latter is obtained by a Monte Carlo calculation, which, starting from the theoretical distribution^{2,3} including form-factor effects, simulates the entire experiment by generating pseudoevents. To these we apply the same analysis procedure as to the experimental events. To the theoretical spectra we add a contribution for our remaining backgrounds; we also estimate radiative-correction effects.

4. RESULTS

A. π^0 Form Factor

The distribution of pairs from Dalitz decay (1) can be written in terms of the π^0 form-factor slope a :

$$f(x, a) = f_0(x)(1 + ax)^2 \approx f_0(x)(1 + 2ax).$$

We see that both the event rate and the shape of the spectrum are dependent on the form factor. Furthermore, it is clear that rate and spectrum shape contain orthogonal information.

Now the systematic errors in determining the spectrum shape are associated with the uncertainty in the energy scale which leaves the absolute-rate determination essentially unaffected. The systematic errors of a in the rate measurement are because of the error in determining the absolute efficiency of our apparatus, which does not affect at all the shape of the spectrum. Therefore, we choose to obtain a separately from the

observed rate of events and from the observed shape of the normalized spectrum. Thus, we have in fact two completely independent measurements; the two determinations of a , starting with orthogonal data, are not coupled by systematic errors either. In comparing the two values we have an internal check of the experiment. Because the results are consistent, we can combine them to obtain the form-factor slope corresponding to the totality of our information.

For the estimate of a from the spectrum shape we use the maximum-likelihood method. We obtain

$$a_{\text{spectrum}} = (-0.10 \pm 0.09)/m_{\pi^0}{}^2,$$

where the error is purely statistical. It is defined as the half-width of the interval of a at whose extremes the logarithm of the likelihood function has decreased by 0.5 from its maximum values. To obtain a from the absolute rate we compare directly the observed number of pairs in the π^0 channel with the expected number calculated by the Monte Carlo method. The result is

$$a_{\text{rate}} = (0.11 \pm 0.07)/m_{\pi^0}{}^2,$$

with the error again only statistical.

The systematic errors in the experiment are due to the uncertainties in the parameters describing the apparatus. These parameters were obtained by measurements during our runs; each of these measurements has an experimental error.

For the spectrum shape the energy scale and the resolution function are both obtained from the γ spectra mentioned in Sec. 2. In particular, we get our gain from the position of the 129-MeV γ peak from radiative capture and the edges of the γ spectrum for $\pi^0 \rightarrow \gamma\gamma$. Our experimental error in this determination is ± 0.3 MeV. The resolution function, obtained from the same spectra, also has an experimental error. These errors, together with the statistical error of our theoretical spectrum (obtained from a finite number of Monte Carlo events) give a systematic error, random in origin, of

$$\delta a_{\text{spectrum}} = \pm 0.13/m_{\pi^0}{}^2.$$

What we call the systematic error in the rate determination is the uncertainty in the expected number of events. This number is given by the product of the event rate per stop (from our Monte Carlo calculation), the number of π^- stops in hydrogen, and the efficiency of our apparatus (scintillation-counter, spark-chamber, camera efficiencies). Associated with the first we have the statistical error of our Monte Carlo events; the number of stops and all efficiencies were measured directly, and each of these measurements had a finite statistical error. The total uncertainty in the expected rate, entirely statistical in origin, is $\pm 5\%$, which translates to a systematic error on the form-factor slope of

$$\delta a_{\text{rate}} = \pm 0.12/m_{\pi^0}{}^2,$$

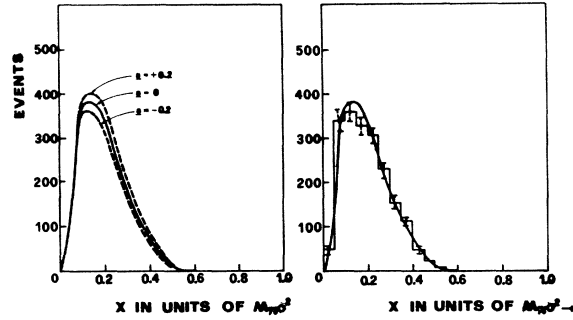


FIG. 10. (a) Theoretical distribution of the invariant mass squared x , obtained for our apparatus with π^0 form-factor slopes $a = -0.2, 0$ and $+0.2$. (b) Histogram of x for our final sample of π^0 decay events, with background subtracted, and the theoretical distribution obtained for our apparatus, with slope $a = +0.01$. The two curves are drawn with equal areas.

the uncertainty in background subtraction being negligible.

The fact that our two values of a have opposite signs is not, we think, disquieting, for these independent results agree within their total errors. We can combine them by taking their weighted average.

For the final error on the result we must combine the statistical and systematic errors of our measurements. Our systematic errors are in fact random or statistical in origin, and, furthermore, they are completely uncorrelated, as are our statistical errors. Therefore, we fulfill the conditions for adding all our errors in quadrature, a procedure which would not be justified for every kind of systematic error. We get

$$a = (+0.01 \pm 0.11)/m_{\pi^0}{}^2,$$

where the purely statistical error is $\pm 0.05/m_{\pi^0}{}^2$.

The agreement between experimental and theoretical distributions (Fig. 10) is checked by a χ^2 test. We find $\chi^2 = 13.5$ for 10 degrees of freedom, corresponding to a 20% confidence level. As a confirmation on our result, we repeat the estimate using only π^0 events with observed γ 's in the lead spark chamber. We obtain, from 997 events, entirely free of background,

$$a_{\gamma} = (-0.03 \pm 0.09)/m_{\pi^0}{}^2.$$

This is completely consistent with the result based on the total sample of 2200 events.

B. Charged Pion Form Factor

Analyzing the pairs from radiative capture (2), we can again get independent estimates of the charged-pion form-factor slope b from the spectrum shape and from the absolute rate. For the spectrum shape we use the minimum χ^2 method and get

$$b_{\text{spectrum}} = (0.55 \pm 0.80)/m_{\pi^-}{}^2,$$

where the error is purely statistical, defined as the half-width of the interval at whose extremes the χ^2 is

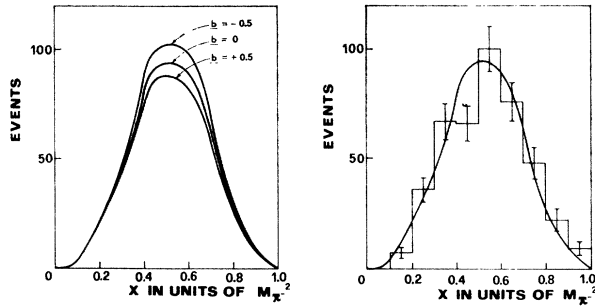


FIG. 11. (a) Theoretical distribution of the invariant mass squared x obtained for our apparatus with π^- form-factor slopes $b = -0.5, 0$ and $+0.5$. (b) Histogram of x for our final sample of radiative capture events and the theoretical distribution obtained for our apparatus, with a slope $b = -0.17$. The two curves are drawn with equal areas.

equal to its minimum value plus one. From the absolute rate we get, by direct comparison with the Monte Carlo calculation,

$$b_{\text{rate}} = (-0.35 \pm 0.29)/m_{\pi}^{-2},$$

where the error is statistical.

The systematic error for the spectrum, due essentially to energy-scale uncertainties, is

$$\delta b_{\text{spectrum}} = \pm 0.2/m_{\pi}^{-2}.$$

For the rate we again have uncertainties in the efficiency that give

$$\delta b_{\text{rate}} = \pm 0.3/m_{\pi}^{-2}.$$

Following exactly our arguments in the case of the π^0 form factor, we combine the two results, with

$$b = (-0.17 \pm 0.37)/m_{\pi}^{-2},$$

where the combined statistical error is $\pm 0.28/m_{\pi}^{-2}$.

The comparison of the observed spectrum shape with the theoretical one, calculated for $b = -0.17$ (Fig. 11), gives $\chi^2 = 10.6$ for five degrees of freedom, corresponding to a 6.5% confidence level.

5. CONCLUSIONS

We summarize the available information on the π^0 form-factor slope a in Table I. Our experiment does not confirm the previously reported large negative values of the form-factor slope and has a somewhat improved associated error. The combined value of the slope obtained by the bubble-chamber experiments was -0.18 . This was difficult to reconcile with a credible model of the interaction. Our form-factor slope agrees with the theoretical expectation.

TABLE I. Available information on the π^0 form-factor slope.

Determination	π^0 form-factor slope	Errors	
		Statistical	Total
Theory, ρ exchange ^a	$a = +0.032$		
Theory, subtracted dispersion relation ^b	$a = +0.046$		
Samios, H ₂ bubble chamber ^c	$a = -0.24$	± 0.12	± 0.16
Kobrak, H ₂ bubble chamber ^{d,e}	$a = -0.15$	± 0.10	
This experiment	$a = +0.01$	± 0.05	± 0.11

^a Reference 7.

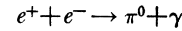
^b Reference 6.

^c Reference 8.

^d Reference 9.

^e The result of Kobrak is given as the slope of the form-factor squares, $2a = -0.3 \pm 0.2$. The error quoted is statistical only, not defined as a standard error. No estimate of systematic errors is given.

A very substantial improvement in accuracy—which is likely to be governed, as in this experiment, by systematic rather than statistical factors—would be necessary to make detailed tests of particular theories. At this level even the question of radiative corrections would need reexamination. For the same purpose, the study of the reaction



with the new storage-ring machines might also be promising.

The only previous knowledge about the charged-pion form-factor slope b was based on measurements of F_{π} in the region of spacelike momentum transfers. The electroproduction experiments^{13,14} are consistent both with the equality $F_{\pi} = G_{E\rho}$, that is $r_{\pi} = 0.81$ F for the pion charge radius, and with the ρ -dominance model, that is $r_{\pi} = 0.63$ F. A recent π -He scattering experiment¹⁶ gives a pion radius $r_{\pi} = 2.96 \pm 0.43$ F. Our result, $b = (-0.17 \pm 0.37)/m_{\pi}^{-2}$, for the slope of F_{π} at small timelike momentum transfers, gives for the radius an upper limit of 1.9 F with a 90% confidence level. Clearly much better measurements are needed even for deciding the simple question of the charge radius.

New important sources of information on F_{π} at large timelike momenta are the e^+e^- storage rings, which have already yielded some very interesting results.^{17,18}

ACKNOWLEDGMENTS

One of us (E.D.C.) wishes to thank Professor L. Lederman for the hospitality of Nevis Laboratories during the main phases of this experiment. We thank K. N. Lee for his contribution to the event-reconstruction program; E. Valente for his contribution to the analysis of the radiative capture channel; Yin Au, who designed most of the equipment; our technicians; the Nevis and Rome scanners; and finally, Bill Hunt and the cyclotron operating crew.